Annales Univ. Sci. Budapest., Sect. Comp. 59 (2026) 25–45

BROADENING THE CONVERGENCE DOMAIN OF THE MODIFIED WEERAKOON–FERNANDO SCHEME FOR EQUATIONS IN BANACH SPACES

Ioannis K. Argyros (Lawton, USA)
Debasis Sharma (Odisha, India)
Christopher Argyros (Atlanta, USA)

Communicated by László Szili
(Received 21 September 2025; accepted 28 February 2026)

Abstract. The effectiveness of iterative schemes in solving nonlinear operator equations heavily depends on the selection of an appropriate initial choice. As a result, accurately estimating the convergence radii and developing theoretical techniques to expand the convergence region are crucial for ensuring the reliability and efficiency of such methods. Local convergence analysis, which focuses on the neighborhood of the exact solution, serves as a vital analytical framework for determining the convergence radii. In this study, we focus on improving the domain of convergence of the modified Weerakoon–Fernando iteration scheme. We conduct a detailed local convergence analysis within the setting of Banach spaces and derive explicit expressions for the convergence radius, error bounds, and the convergence zones associated with this scheme. A key feature of the proposed approach is that it depends only on the first derivative and does not require any extra conditions, which simplifies implementation while substantially enlarging the convergence domain compared to existing techniques. The theoretical advancements are substantiated through a series of rigorous numerical experiments applied to a variety of nonlinear problems. Additionally, the analysis of attraction basins offers further insights into the method's dynamic behavior, stability, and suitability for solving complex polynomial equations.

Key words and phrases: Banach space, local convergence, nonlinear equations, Newton-like methods, generalized Lipschitz–Hölder-type conditions.
2010 Mathematics Subject Classification: 47J25, 49M15, 65J15, 65H99.
https://doi.org/10.71352/ac.59.280226

1. Introduction

Across many areas of applied science and engineering, practitioners frequently encounter nonlinear operator equations of the kind

$$\widehat{\zeta}(b) = 0, \tag{1.1}$$

where $\widehat{\zeta} : \widetilde{\mathcal{D}} \subseteq \widetilde{\mathcal{D}}_1 \to \widetilde{\mathcal{D}}_2$ is a continuously Fréchet derivable operator, $\widetilde{\mathcal{D}}_m$'s are Banach spaces for $m = 1, 2$, and $\widetilde{\mathcal{D}} \subseteq \widetilde{\mathcal{D}}_1$ is both open and convex. It is widely recognized that, in general, analytical techniques are insufficient to obtain exact solutions to (1.1). Consequently, one must rely on iterative schemes to generate approximate solutions. Among such schemes, Newton's method (NM) is considered one of the most influential iterative techniques for solving (1.1). This scheme appears as follows

$$b_{s+1} = b_s - \widehat{\zeta}'(b_s)^{-1}\widehat{\zeta}(b_s), \ s \in \mathbb{N} \cup \{0\}. \tag{1.2}$$

Renowned for its computational effectiveness and quadratic convergence, Newton's scheme has long served as a foundational tool for the development of various higher-order iterative schemes [4, 13, 16, 18, 19, 20, 22, 28, 29]. Weerakoon and Fernando [29] created the following third-order iteration scheme by modifying NM

$$\begin{aligned} p_s &= b_s - \widehat{\zeta}'(b_s)^{-1}\widehat{\zeta}(b_s), \\ b_{s+1} &= b_s - 2\left[\widehat{\zeta}'(b_s) + \widehat{\zeta}'(p_s)\right]^{-1}\widehat{\zeta}(b_s), \ s \in \mathbb{N} \cup \{0\}. \end{aligned} \tag{1.3}$$

Later, Cordero et al. [13] extended this scheme (1.3) to introduce the fifth-order modified Weerakoon–Fernando iterative method (MWFM). This method is structured as follows

$$\begin{aligned} p_s &= b_s - \widehat{\zeta}'(b_s)^{-1}\widehat{\zeta}(b_s), \\ \eta_s &= b_s - 2\left[\widehat{\zeta}'(b_s) + \widehat{\zeta}'(p_s)\right]^{-1}\widehat{\zeta}(b_s), \\ b_{s+1} &= \eta_s - \widehat{\zeta}'(p_s)^{-1}\ \widehat{\zeta}(\eta_s), \ s \in \mathbb{N} \cup \{0\}. \end{aligned} \tag{1.4}$$

More recently, a significant focus has been placed on removing the dependency on Taylor series in the convergence analysis of iterative schemes. Researchers, including Amat et al. [1], Argyros et al. [3, 6, 5, 7, 8, 9, 10], Cordero et al. [12], Hernández–Verón et al. [14], and George et al. [15], have explored the local and semi-local convergence properties of iterative techniques with fourth or higher orders of convergence. Similarly, various researchers [23, 24, 26] broadened the practical usefulness of MWFM by conducting its local convergence analysis, utilizing the Lipschitz and Hölder continuity of $\widehat{\zeta}'$. In addition,

Martínez et al. [17], Chang et al. [11], and others [21, 25, 27] contributed to developing convergence theories independent of higher-order derivatives.

When working with iterative schemes, another key challenge is identifying the domain where the method actually converges. Often, this domain is quite narrow. Expanding the convergence domain, without relying on additional assumptions, is therefore an important goal. We perform a rigorous local convergence analysis of MWFM [13] within the context of Banach spaces, deriving precise expressions for the convergence radius, error bounds, and the convergence regions associated with MWFM. Our analysis employs the generalized Lipschitz-Hölder–type continuity conditions imposed on the first derivative of $\widehat{\zeta}$, and supported by some auxiliary functions. The theoretical findings are reinforced through systematic numerical experiments conducted on a broad spectrum of nonlinear problems. Additionally, we address the following issues for MWFM.

($\delta 1$) The convergence of MWFM is established in [13] using Taylor series expansions which require the existence of higher-order derivatives not present on the method (see also the problems on the numerical section 4).

($\delta 2$) There are no a priori error estimates on the distances. So, we do not know in advance the required number of iterations to be carried out to reach a desired error tolerance $\epsilon > 0$.

($\delta 3$) There is no information on the isolation of the solution.

($\delta 4$) The local convergence analysis in [13] is valid for mappings defined on the finite dimensional Euclidean space.

Issues ($\delta 1$)–($\delta 4$) constitute our motivation for this paper, which are addressed positively as follows:

($\delta' 1$) The new convergence analysis is shown using only the operators on the method, i.e. the operator and its derivative.

($\delta' 2$) We do know the number of iterates to be carried out in advance, since a priori estimates are provided.

($\delta' 3$) A domain is specified that contains only one solution of the nonlinear equation (1.1).

($\delta' 4$) The convergence is established in the more general setting of a Banch space.

Therefore, we broaden the applicability of the method under weaker sufficient convergence conditions. Our analysis also leads to a considerable expansion of the convergence domain of MWFM when compared to existing techniques [23, 24, 26]. Moreover, a graphical investigation of the method's attraction basins provides additional understanding of its dynamic behavior, robustness, and applicability to solving complex polynomial equations.

The structure of this work is as follows: Section 2 presents the theoretical framework for local convergence of MWFM within Banach spaces. Section 3 uses attraction basin analysis to assess the stability and convergence characteristics of MWFM. Section 4 includes comprehensive numerical experiments

to confirm the practical advantages of our theoretical approach. Conclusions are listed in Section 5.

2. Analysis of local convergence

This section takes an in-depth look into the local convergence of the iterative technique MWFM. We begin our discussion by designing the following notations. Let

$$P(t,c^*) := \{b \in \widetilde{\mathcal{D}}_1 \mid ||t-b|| < c^*\},$$
$$P[t,c^*] := \{b \in \widetilde{\mathcal{D}}_1 \mid ||t-b|| \leq c^*\}, \quad t \in \widetilde{\mathcal{D}}_1 \text{ and } c^* > 0,$$
$$\mathcal{L}_B(\widetilde{\mathcal{D}}_1, \widetilde{\mathcal{D}}_2) := \{\overline{\mathcal{B}} : \widetilde{\mathcal{D}}_1 \to \widetilde{\mathcal{D}}_2 \mid \overline{\mathcal{B}} \text{ is bounded and linear}\}, \text{ and } \mathcal{V} := [0,\infty)$$

Suppose that $\widehat{\zeta} : \widetilde{\mathcal{D}} \subseteq \widetilde{\mathcal{D}}_1 \to \widetilde{\mathcal{D}}_2$ possesses the following properties.

(Θ1) $\widehat{\zeta}$ is continuously Fréchet derivable,

(Θ2) $\widehat{\zeta}(\widehat{u}_*) = 0$, $\widehat{u}_* \in \widetilde{\mathcal{D}}$,

(Θ3) $\widehat{\zeta}'(\widehat{u}_*)^{-1} \in \mathcal{L}_B(\widetilde{\mathcal{D}}_2, \widetilde{\mathcal{D}}_1)$,

(Θ4) $||\widehat{\zeta}'(\widehat{u}_*)^{-1}(\widehat{\zeta}'(b) - \widehat{\zeta}'(\widehat{u}_*))|| \leq \widehat{\mathcal{P}}_0(||b - \widehat{u}_*||)$, $\forall b \in \widetilde{\mathcal{D}}$, and

(Θ5) $||\widehat{\zeta}'(\widehat{u}_*)^{-1}(\widehat{\zeta}'(b) - \widehat{\zeta}'(u))|| \leq \widehat{\mathcal{P}}(||b-u||)$, $\forall b, u \in \widetilde{\mathcal{D}}_0 := \widetilde{\mathcal{D}} \cap P(\widehat{u}_*, \kappa_0)$,

where $\widehat{\mathcal{P}} : \mathcal{V} \to \mathcal{V}$ and $\widehat{\mathcal{P}}_0 : \mathcal{V} \to \mathcal{V}$ are continuous and non-decreasing functions such that

(E1) $\widehat{\mathcal{P}}(0) = \widehat{\mathcal{P}}_0(0) = 0$, and

(E2) there exists the smallest real number, $\kappa_0 > 0$, that solves $\widehat{\mathcal{P}}_0(\sigma) - 1 = 0$.

Now, we introduce functions Ω_m and $\widehat{\chi}_m$ for $m = 1, 2, 3$, defined on $[0, \kappa_0)$ by

$$\Omega_1(\sigma) = \frac{\int_0^1 \widehat{\mathcal{P}}((1-\varpi)\sigma)\, d\varpi}{1 - \widehat{\mathcal{P}}_0(\sigma)}, \tag{2.1}$$

$$\Omega_2(\sigma) = \frac{1}{2}\left[\widehat{\mathcal{P}}_0(\sigma) + \widehat{\mathcal{P}}_0(\Omega_1(\sigma)\sigma)\right], \tag{2.2}$$

$$\Omega_3(\sigma) = \widehat{\mathcal{P}}_0(\Omega_1(\sigma)\sigma), \tag{2.3}$$

and

$$\widehat{\chi}_m(\sigma) = \Omega_m(\sigma) - 1. \tag{2.4}$$

Then, $\lim_{\sigma\to\kappa_0^-}\widehat{\chi}_1(\sigma)=+\infty$ and $\widehat{\chi}_1(0)<0$. Consequently, $(0,\kappa_0)$ contains at least one real number that solves $\widehat{\chi}_1(\sigma)=0$. Suppose that $\kappa_m\in(0,\kappa_0)$ be the least real number that solves the equation $\widehat{\chi}_m(\sigma)=0$ for $m=1,2,3$. We construct Ω_4 and $\widehat{\chi}_4$ on $[0,\kappa_2)$ by

$$\Omega_4(\sigma)=\frac{\left[\int_0^1\widehat{\mathcal{P}}((1-\varpi)\sigma)\;d\varpi+\int_0^1\widehat{\mathcal{P}}(\Omega_1(\sigma)\sigma+\varpi\sigma)\;d\varpi\right]}{2(1-\Omega_2(\sigma))},\tag{2.5}$$

and

$$\widehat{\chi}_4(\sigma)=\Omega_4(\sigma)-1.\tag{2.6}$$

Then, $\lim_{\sigma\to\kappa_2^-}\widehat{\chi}_4(\sigma)=+\infty$ and $\widehat{\chi}_4(0)=-1<0$. So, the minimal solution κ_4 of $\widehat{\chi}_4(\sigma)=0$ is contained in $(0,\kappa_2)$. Finally, we construct Ω_5 and $\widehat{\chi}_5$ on $[0,\kappa_3)$ by

$$\Omega_5(\sigma)=\frac{\int_0^1\widehat{\mathcal{P}}(\Omega_1(\sigma)\sigma+\varpi\Omega_4(\sigma)\sigma)\;d\varpi\;\Omega_4(\sigma)}{(1-\Omega_3(\sigma))}\tag{2.7}$$

and

$$\widehat{\chi}_5(\sigma)=\Omega_5(\sigma)-1.\tag{2.8}$$

Then, $\lim_{\sigma\to\kappa_3^-}\widehat{\chi}_5(\sigma)=+\infty$ and $\widehat{\chi}_5(0)=-1<0$. Let $\kappa_5\in(0,\kappa_3)$ be the least real number that satisfies $\widehat{\chi}_5(\sigma)=0$. Notice that, for $0\leq\sigma<\widehat{R}^*$ and $m=1,2,\ldots,5$, we have

$$\Omega_m(\sigma)\in[0,1),\tag{2.9}$$

where the radius $\widehat{R}^*$ is given by

$$\widehat{R}^*=min\{\kappa_1,\kappa_4,\kappa_5\}.\tag{2.10}$$

Next, we establish the local convergence theorem for MWFM in Theorem 1.

Theorem 2.1. *Suppose that for $\widehat{\zeta}:\widetilde{\mathcal{D}}\subseteq\widetilde{\mathcal{D}}_1\to\widetilde{\mathcal{D}}_2$, the conditions* (Θ1)–(Θ5) *are true. Let $P[\widehat{u}_*,\widehat{R}^*]\subseteq\widetilde{\mathcal{D}}$ and $\int_0^1\widehat{\mathcal{P}}_0(\varpi\widehat{R})\;d\varpi<1$ for some $\widehat{R}\geq\widehat{R}^*$. Let MWFM produces $\{b_s\}$, the sequence of iterates, starting with $b_0\in P(\widehat{u}_*,\widehat{R}^*)$. Then,*

(i) $\{b_s\}$ *is well defined,*

(ii) $\{b_s\}\in P(\widehat{u}_*,\widehat{R}^*)$, *and*

(iii) $\lim_{s\to\infty}b_s=\widehat{u}_*$.

Furthermore, for $s \in \mathbb{N} \cup \{0\}$, we deduce that

$$||p_s - \widehat{u}_*|| \leq \Omega_1(||b_s - \widehat{u}_*||)||b_s - \widehat{u}_*|| < ||b_s - \widehat{u}_*|| < \widehat{R}^*, \tag{2.11}$$

$$||\eta_s - \widehat{u}_*|| \leq \Omega_4(||b_s - \widehat{u}_*||)||b_s - \widehat{u}_*|| < ||b_s - \widehat{u}_*|| < \widehat{R}^* \quad \textit{and} \tag{2.12}$$

$$||b_{s+1} - \widehat{u}_*|| \leq \Omega_5(||b_s - \widehat{u}_*||)||b_s - \widehat{u}_*|| < ||b_s - \widehat{u}_*|| < \widehat{R}^*, \tag{2.13}$$

where Ω_1, Ω_4, Ω_5, and $\widehat{R}^*$ are provided in (2.1), (2.5), (2.7) and (2.10), respectively. Additionally, $\widehat{u}_*$ is the only possible solution of (1.1) in $P[\widehat{u}_*, \widehat{R}] \cap \widetilde{\mathcal{D}}$.

Proof. Our primary intent is to deduce (2.11)-–(2.13) when $s = 0$. The assumption that $b_0 \in P(\widehat{u}_*, \widehat{R}^*)$, along with condition ($\Theta$4) and equation (2.10), yields that

$$||\widehat{\zeta}'(\widehat{u}_*)^{-1}(\widehat{\zeta}'(b_0) - \widehat{\zeta}'(\widehat{u}_*))|| \leq \widehat{\mathcal{P}}_0(||b_0 - \widehat{u}_*||) < \widehat{\mathcal{P}}_0(\widehat{R}^*) < 1. \tag{2.14}$$

We apply a lemma given by Banach on invertible operators [2, 4, 28] to confirm that $\widetilde{\zeta}'(b_0)^{-1} \in \mathcal{L}_B(\widetilde{\mathcal{D}}_2, \widetilde{\mathcal{D}}_1)$. Also, we have

$$||\widehat{\zeta}'(b_0)^{-1}\widehat{\zeta}'(\widehat{u}_*)|| \leq \frac{1}{1 - \widehat{\mathcal{P}}_0(||b_0 - \widehat{u}_*||)} < \frac{1}{1 - \widehat{\mathcal{P}}_0(\widehat{R}^*)}. \tag{2.15}$$

Consequently, setting $s = 0$ in (1.4) confirms the existence of p_0. Again, putting $s = 0$ in the first equation $p_s = b_s - \widehat{\zeta}'(b_s)^{-1}\widehat{\zeta}(b_s)$ of (1.4), we have

$$\begin{aligned} p_0 - \widehat{u}_* &= b_0 - \widehat{u}_* - \widehat{\zeta}'(b_0)^{-1}\widehat{\zeta}(b_0) = \\ &= -\left[\widehat{\zeta}'(b_0)^{-1}\widehat{\zeta}'(\widehat{u}_*)\right] \times \\ &\times \left[\int_0^1 \widehat{\zeta}'(\widehat{u}_*)^{-1}(\widehat{\zeta}'(\widehat{u}_* + \varpi(b_0 - \widehat{u}_*)) - \widehat{\zeta}'(b_0))(b_0 - \widehat{u}_*)d\varpi\right]. \end{aligned} \tag{2.16}$$

Using (Θ5) (see page 28), (2.1), (2.9), (2.10) and (2.15) in (2.16), we get

$$\begin{aligned} ||p_0 - \widehat{u}_*|| &\leq \left[||\widehat{\zeta}'(b_0)^{-1}\widehat{\zeta}'(\widehat{u}_*)||\right] \times \\ &\times \left[\left|\left|\int_0^1 \widehat{\zeta}'(\widehat{u}_*)^{-1}(\widehat{\zeta}'(\widehat{u}_* + \varpi(b_0 - \widehat{u}_*)) - \widehat{\zeta}'(b_0))(b_0 - \widehat{u}_*)\, d\varpi\right|\right|\right] \leq \\ &\leq \frac{\int_0^1 \widehat{\mathcal{P}}((1-\varpi)||b_0 - \widehat{u}_*||)\, d\varpi ||b_0 - \widehat{u}_*||}{(1 - \widehat{\mathcal{P}}_0(||b_0 - \widehat{u}_*||))} = \\ &= \Omega_1(||b_0 - \widehat{u}_*||)||b_0 - \widehat{u}_*|| < ||b_0 - \widehat{u}_*|| < \widehat{R}^*, \end{aligned} \tag{2.17}$$

and this confirms that (2.11) is true for $s = 0$. Then, we wish to deduce that $[\widehat{\zeta}'(b_0) + \widehat{\zeta}'(p_0)]^{-1} \in \mathcal{L}_B(\widetilde{\mathcal{D}}_2, \widetilde{\mathcal{D}}_1)$. The condition (Θ_4) (see page 28) and equations (2.2), (2.9), (2.10), and (2.17) are employed to derive that

$$\begin{aligned}
&||(2\widehat{\zeta}'(\widehat{u}_*))^{-1}(\widehat{\zeta}'(b_0) + \widehat{\zeta}'(p_0) - 2\widehat{\zeta}'(\widehat{u}_*))|| \leq \\
&\leq \frac{1}{2}[||\widehat{\zeta}'(\widehat{u}_*)^{-1}(\widehat{\zeta}'(b_0) - \widehat{\zeta}'(\widehat{u}_*))|| + ||\widehat{\zeta}'(\widehat{u}_*)^{-1}(\widehat{\zeta}'(p_0) - \widehat{\zeta}'(\widehat{u}_*))||] \leq \\
&\leq \frac{1}{2}\left[\widehat{\mathcal{P}}_0(||b_0 - \widehat{u}_*||) + \widehat{\mathcal{P}}_0(||p_0 - \widehat{u}_*||)\right] \leq \\
&\leq \frac{1}{2}\left[\widehat{\mathcal{P}}_0(||b_0 - \widehat{u}_*||) + \widehat{\mathcal{P}}_0(\Omega_1(||b_0 - \widehat{u}_*||)||b_0 - \widehat{u}_*||)\right] = \\
&= \Omega_2(||b_0 - \widehat{u}_*||) < \Omega_2(\widehat{R}^*) < 1.
\end{aligned}$$

Consequently, $[\widehat{\zeta}'(b_0) + \widehat{\zeta}'(p_0)]^{-1} \in \mathcal{L}_B(\widetilde{\mathcal{D}}_2, \widetilde{\mathcal{D}}_1)$ and η_0 exists. Also,

$$||[\widehat{\zeta}'(b_0) + \widehat{\zeta}'(p_0)]^{-1}\widehat{\zeta}'(\widehat{u}_*)|| \leq \frac{1}{2(1 - \Omega_2(||b_0 - \widehat{u}_*||))}. \tag{2.18}$$

Next, we shall confirm that $\widehat{\zeta}'(p_0)$ is invertible. From $(\Theta 4)$ (see page 28), (2.3), (2.9), (2.10), and (2.17), we get

$$\begin{aligned}
||\widehat{\zeta}'(\widehat{u}_*)^{-1}(\widehat{\zeta}'(p_0) - \widehat{\zeta}'(\widehat{u}_*))|| &\leq \widehat{\mathcal{P}}_0(||p_0 - \widehat{u}_*||) \leq \\
&\leq \widehat{\mathcal{P}}_0(\Omega_1(||b_0 - \widehat{u}_*||)||b_0 - \widehat{u}_*||) = \\
&= \Omega_3(||b_0 - \widehat{u}_*||) < \Omega_3(\widehat{R}^*) < 1. \qquad (2.19)
\end{aligned}$$

This inequality yields $\widehat{\zeta}'(p_0)^{-1} \in \mathcal{L}_B(\widetilde{\mathcal{D}}_2, \widetilde{\mathcal{D}}_1)$ and

$$||\widehat{\zeta}'(p_0)^{-1}\widehat{\zeta}'(\widehat{u}_*)|| \leq \frac{1}{1 - \Omega_3(||b_0 - \widehat{u}_*||)}. \tag{2.20}$$

As a result, b_1 exists. We put $s = 0$ in the second equation of (1.4) and use $(\Theta 5)$ (see page 28), (2.5), (2.9), (2.10), (2.17), and (2.18) to produce

$$\begin{aligned}
&||\eta_0 - \widehat{u}_*|| \leq \left(||[\widehat{\zeta}'(b_0) + \widehat{\zeta}'(p_0)]^{-1}\widehat{\zeta}'(\widehat{u}_*)||\right) \times \\
&\times \left(\left|\left|\int_0^1 \widehat{\zeta}'(\widehat{u}_*)^{-1}\left(\widehat{\zeta}'(b_0) - \widehat{\zeta}'(\widehat{u}_* + \varpi(b_0 - \widehat{u}_*))\right)(b_0 - \widehat{u}_*)d\varpi\right|\right| + \right. \\
&\left. + \left|\left|\int_0^1 \widehat{\zeta}'(\widehat{u}_*)^{-1}\left(\widehat{\zeta}'(p_0) - \widehat{\zeta}'(\widehat{u}_* + \varpi(b_0 - \widehat{u}_*))\right)(b_0 - \widehat{u}_*)d\varpi\right|\right|\right) \leq \\
&\leq \frac{1}{2(1 - \Omega_2(||b_0 - \widehat{u}_*||))} \times \left[\int_0^1 \widehat{\mathcal{P}}((1 - \varpi)||b_0 - \widehat{u}_*||)\, d\varpi||b_0 - \widehat{u}_*|| + \right.
\end{aligned}$$

$$+\int_0^1 \widehat{\mathcal{P}}(||p_0-\widehat{u}_*||+\varpi||b_0-\widehat{u}_*||)\ d\varpi||b_0-\widehat{u}_*||\leq$$

$$\leq \frac{1}{2(1-\Omega_2(||b_0-\widehat{u}_*||))}\times\left[\int_0^1 \widehat{\mathcal{P}}((1-\varpi)||b_0-\widehat{u}_*||)\ d\varpi||b_0-\widehat{u}_*||+\right.$$

$$\left.+\int_0^1 \widehat{\mathcal{P}}(\Omega_1(||b_0-\widehat{u}_*||)||b_0-\widehat{u}_*||+\varpi||b_0-\widehat{u}_*||)\ d\varpi||b_0-\widehat{u}_*||\right]=$$

$$=\frac{1}{2(1-\Omega_2(||b_0-\widehat{u}_*||))}\times\left[\int_0^1 \widehat{\mathcal{P}}((1-\varpi)||b_0-\widehat{u}_*||)\ d\varpi+\right.$$

$$\left.+\int_0^1 \widehat{\mathcal{P}}(\Omega_1(||b_0-\widehat{u}_*||)||b_0-\widehat{u}_*||+\varpi||b_0-\widehat{u}_*||)\ d\varpi\right]||b_0-\widehat{u}_*||=$$

$$=\Omega_4(||b_0-\widehat{u}_*||)||b_0-\widehat{u}_*||<||b_0-\widehat{u}_*||<\widehat{R}^*. \tag{2.21}$$

Hence, (2.12) holds true for $s=0$. Finally, to establish (2.13), we set $s=0$ in the last equation $b_{s+1}=\eta_s-\widehat{\zeta}'(p_s)^{-1}\ \widehat{\zeta}(\eta_s)$ of (1.4) and yield

$$b_1-\widehat{u}_*=\eta_0-\widehat{u}_*-\widehat{\zeta}'(p_0)^{-1}\widehat{\zeta}(\eta_0)= \tag{2.22}$$

$$=-[\widehat{\zeta}'(p_0)^{-1}\widehat{\zeta}'(\widehat{u}_*)]\left[\int_0^1 \widehat{\zeta}'(\widehat{u}_*)^{-1}(\widehat{\zeta}'(\widehat{u}_*+\varpi(\eta_0-\widehat{u}_*))-\widehat{\zeta}'(p_0))(\eta_0-\widehat{u}_*)d\varpi\right].$$

Therefore, we derive using ($\Theta 5$) (see page 28), (2.7), (2.9), (2.10), (2.17), (2.20), (2.21), and (2.22) that

$$||b_1-\widehat{u}_*||\leq\left[||\widehat{\zeta}'(p_0)^{-1}\widehat{\zeta}'(\widehat{u}_*)||\right]\times$$

$$\times\left[\left|\left|\int_0^1 \widehat{\zeta}'(\widehat{u}_*)^{-1}(\widehat{\zeta}'(\widehat{u}_*+\varpi(\eta_0-\widehat{u}_*))-\widehat{\zeta}'(p_0))(\eta_0-\widehat{u}_*)\ d\varpi\right|\right|\right]\leq$$

$$\leq\frac{\int_0^1 \widehat{\mathcal{P}}(||p_0-\widehat{u}_*||+\varpi||\eta_0-\widehat{u}_*||)\ d\varpi||\eta_0-\widehat{u}_*||}{(1-\Omega_3(||b_0-\widehat{u}_*||))}\leq$$

$$\leq\frac{\int_0^1 \widehat{\mathcal{P}}(\Omega_1(||b_0-\widehat{u}_*||)||b_0-\widehat{u}_*||+\varpi\Omega_4(||b_0-\widehat{u}_*||)||b_0-\widehat{u}_*||)\ d\varpi}{(1-\Omega_3(||b_0-\widehat{u}_*||))}\times$$

$$\times\,\Omega_4(||b_0-\widehat{u}_*||)||b_0-\widehat{u}_*||=$$

$$=\Omega_5(||b_0-\widehat{u}_*||)||b_0-\widehat{u}_*||<||b_0-\widehat{u}_*||<\widehat{R}^*. \tag{2.23}$$

The above inequality guarantees that (2.13) is true for $s=0$. We replace the terms b_0, p_0, η_0, and b_1 by b_s, p_s, η_s, and b_{s+1}, respectively in the earlier computations, and then utilize mathematical induction to produce (2.11)–(2.13)

for $s \geq 1$. Furthermore, the inequality $||b_{s+1} - \widehat{u}_*|| \leq \Omega_5(\widehat{R}^*)||b_s - \widehat{u}_*|| < \widehat{R}^*$ is employed to derive that $b_{s+1} \in P(\widehat{u}_*, \widehat{R}^*)$ and $b_s \to \widehat{u}_*$ as $s \to \infty$.

With the intention of verifying the uniqueness of $\widehat{u}_*$, we assume that $\widehat{\zeta}(\bar{u}^*) = 0$, where $\bar{u}^* \in P[\widehat{u}_*, \widehat{R}] \cap \widetilde{\mathcal{D}}$. Then, for $\widehat{U} = \int_0^1 \mathcal{F}\, d\varpi$, where $\mathcal{F} = \widehat{\zeta}'(\widehat{u}_* + \varpi(\bar{u}^* - \widehat{u}_*))$, we derive

$$\widehat{\zeta}(\widehat{u}_*) - \widehat{\zeta}(\bar{u}^*) = \widehat{U}(\widehat{u}_* - \bar{u}^*) = 0. \tag{2.24}$$

Also, we obtain using (Θ4) (see page 28) that

$$\begin{aligned} ||\widehat{\zeta}'(\widehat{u}_*)^{-1}(\widehat{U} - \widehat{\zeta}'(\widehat{u}_*))|| &\leq \int_0^1 \widehat{\mathcal{P}}_0(||\widehat{u}_* + \varpi(\bar{u}^* - \widehat{u}_*) - \widehat{u}_*||)\, d\varpi = \\ &= \int_0^1 \widehat{\mathcal{P}}_0(\varpi||\bar{u}^* - \widehat{u}_*||)\, d\varpi \leq \\ &\leq \int_0^1 \widehat{\mathcal{P}}_0(\varpi\widehat{R})\, d\varpi < 1. \end{aligned}$$

Hence,

$$\widehat{U}^{-1} \in \mathcal{L}_B(\widetilde{\mathcal{D}}_2, \widetilde{\mathcal{D}}_1). \tag{2.25}$$

Thus, from (2.24) and (2.25), we conclude that $\widehat{u}_* = \bar{u}^*$. ■

3. Basins of attraction

This section explores the convergence behavior and stability properties of MWFM by examining its basins of attraction through graphical simulations. The basin of attraction, also referred to as the Fatou set, is defined as the collection $\{\alpha_0 \in \mathbb{C} : \alpha_m \to \alpha^* \; as \; m \to \infty\}$, where $\breve{\mathcal{H}} : \mathbb{C} \to \mathbb{C}$ is a polynomial, α^* is one of its roots, and $\{\alpha_m\}_{m=0}^{\infty}$ represents the sequence generated by MWFM, beginning from the initial guess $\alpha_0 \in \mathbb{C}$. The Julia set is defined as the complement of this Fatou set. To visualize these attraction regions, a region $\mathcal{Z} = [-4, 4] \times [-4, 4] \subset \mathbb{C}$ is selected and discretized into a 400×400. This allows for the graphical representation of the convergence domains associated with MWFM when applied to different complex polynomial equations, all of whose roots are situated within $\mathcal{Z}$. Each grid point acts as an initial guess for MWFM, which is then applied to six functions provided in Examples (1-3). If the generated sequence converges to a particular root, that initial point is assigned to the corresponding basin of attraction and is color-coded accordingly. The color intensity, from light to dark, reflects the number of iterations needed to reach the root. Points for which the method fails to converge within the

specified criteria are shown in black. The iterative process is capped at 500 iterations, or it stops earlier if the approximation error falls below 10^{-6}. All visualizations have been produced using MATLAB.

Example 1. To explore the basins of attraction, we consider the following cubic polynomials.

(i) $\check{\mathcal{H}}_1(\alpha) = \alpha^3 + 1$.

(ii) $\check{\mathcal{H}}_2(\alpha) = 4\alpha^3 - 3\alpha$.

Figures 1(a) and 1(b) display the graphical representation of the attraction basins for the roots of the polynomials $\check{\mathcal{H}}_1(\alpha)$ and $\check{\mathcal{H}}_2(\alpha)$, respectively. In the case of $\check{\mathcal{H}}_1(\alpha)$, the basins leading to the roots $\frac{1}{2} + 0.866025i$, -1, and $\frac{1}{2} - 0.866025i$ are highlighted in green, cyan, and purple, respectively. Similarly, for the Chebyshev polynomial $\check{\mathcal{H}}_2(\alpha)$, the colors green, orange, and purple correspond to the basins of attraction for the roots 0, $\frac{\sqrt{3}}{2}$, and $-\frac{\sqrt{3}}{2}$, respectively. From the visual analysis in Figure 1, it is evident that the black regions, representing the Julia set, occupy less space in the case of $\check{\mathcal{H}}_2(\alpha)$, indicating a more stable behavior of MWFM when applied to solving $\check{\mathcal{H}}_2(\alpha) = 0$, compared to its performance on $\check{\mathcal{H}}_1(\alpha) = 0$.

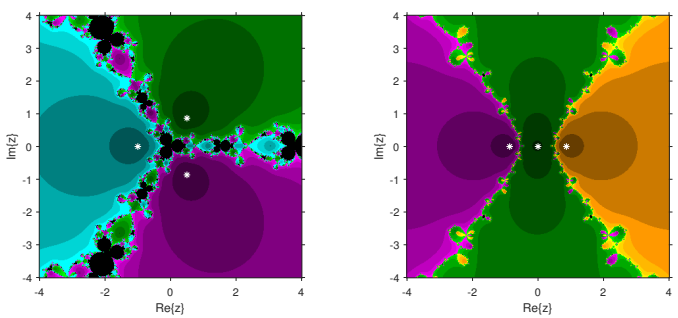

(a) $\check{\mathcal{H}}_1(\alpha)$ (b) $\check{\mathcal{H}}_2(\alpha)$

Figure 1. Basins of attraction corresponding to Example 1

Example 2. We investigate the basins of attraction by analyzing the following quartic polynomials.

(i) $\check{\mathcal{H}}_3(\alpha) = \alpha^4 - 3\alpha^3 + 3\alpha^2 - 3\alpha + 2$.

(ii) $\check{\mathcal{H}}_4(\alpha) = 8\alpha^4 - 8\alpha^2 + 1$.

Figures 2(a) and 2(b) illustrate the basins of attraction corresponding to the roots of the polynomials $\check{\mathcal{H}}_3(\alpha)$ and $\check{\mathcal{H}}_4(\alpha)$, respectively. For $\check{\mathcal{H}}_3(\alpha)$, the basins associated with the roots $-i$, 1, i, and 2 are depicted in purple, green, red, and orange, respectively. In the case of the Chebyshev polynomial $\check{\mathcal{H}}_4(\alpha)$, the

regions leading to the roots $-\sqrt{\frac{2-\sqrt{2}}{4}}$, $\sqrt{\frac{2-\sqrt{2}}{4}}$, $-\sqrt{\frac{2+\sqrt{2}}{4}}$, and $\sqrt{\frac{2+\sqrt{2}}{4}}$ are shaded orange, purple, green, and cyan, respectively. It can be observed from Figure 2 that the black area, representing the Julia set, is significantly smaller for $\check{\mathcal{H}}_4(\alpha)$, suggesting that MWFM provides improved stability when applied to $\check{\mathcal{H}}_4(\alpha) = 0$ compared to its application to $\check{\mathcal{H}}_3(\alpha) = 0$.

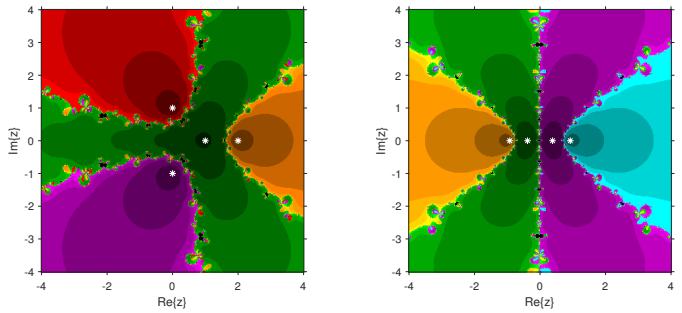

(a) $\check{\mathcal{H}}_3(\alpha)$ (b) $\check{\mathcal{H}}_4(\alpha)$

Figure 2. Basins of attraction corresponding to Example 2

Example 3. The structure of basins of attraction is explored for the following of polynomials of degree five.

(i) $\check{\mathcal{H}}_5(\alpha) = \alpha^5 - 2\alpha^4 - (1+2i)\alpha^3 + (2+4i)\alpha^2 + 2i\alpha - 4i.$

(ii) $\check{\mathcal{H}}_6(\alpha) = 16\alpha^5 - 20\alpha^3 + 5\alpha.$

Figures 3(a) and 3(b) depict the attraction basins associated with the roots of the polynomials $\check{\mathcal{H}}_5(\alpha)$ and $\check{\mathcal{H}}_6(\alpha)$, respectively. For $\check{\mathcal{H}}_5(\alpha)$, the convergence regions corresponding to the roots -1, $1+i$, 1, $-(1+i)$, and 2 are shown in blue, red, purple, yellow, and green, respectively. Likewise, the basins for the roots $-\sqrt{\frac{5-\sqrt{5}}{8}}$, $-\sqrt{\frac{5+\sqrt{5}}{8}}$, 0, $\sqrt{\frac{5-\sqrt{5}}{8}}$, and $\sqrt{\frac{5+\sqrt{5}}{8}}$ of the Chebyshev polynomial $\check{\mathcal{H}}_6(\alpha)$ are represented using green, red, orange, blue, and purple shading, respectively. It is confirmed from the plots that the black region, denoting the Julia set, is noticeably smaller for $\check{\mathcal{H}}_6(\alpha)$. This observation suggests that MWFM exhibits improved stability and convergence properties when applied to $\check{\mathcal{H}}_6(\alpha) = 0$ compared to its behavior on $\check{\mathcal{H}}_5(\alpha) = 0$.

4. Numerical validation of the proposed analysis

To support the theoretical outcomes developed in Section 2, this section presents a series of computational experiments. Specifically, for each of Problems 1 to 5, we implement the proposed procedure to evaluate the radii associated with MWFM. The calculation process incorporates the use of functions Ω_m, $m = 1, 2, 3, 4, 5$, which play a central role in quantifying the radii. The

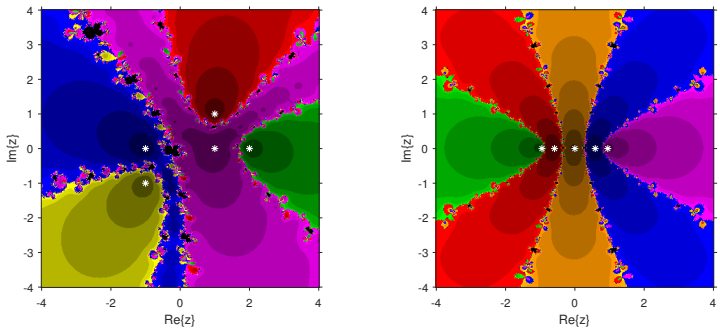

(a) $\check{\mathcal{H}}_5(\alpha)$ (b) $\check{\mathcal{H}}_6(\alpha)$

Figure 3. Basins of attraction corresponding to Example 3

complete set of numerical results is compiled and displayed in Tables 1–5. These results distinctly indicate that the radii of MWFM, achieved through our proposed technique, are significantly larger than those reported in prior studies [23, 24, 26]. In the Tables (1-5), $**$ represents that the parameter cannot be determined. In Figures 4–8, the functions Ω_m, $m = 1, 2, ..., 5$, are displayed to graphically illustrate that $0 \leq \Omega_m(\sigma) < 1$ when $\sigma \in (0, \widehat{R}^*)$.

Problem 1. [24] Suppose that $\widetilde{\mathcal{D}}_1 = \widetilde{\mathcal{D}}_2 = \mathbb{R}$ and $\widetilde{\mathcal{D}} = [-\frac{1}{2}, \frac{3}{2}]$. Then, for $\widehat{\zeta} : \widetilde{\mathcal{D}} \to \mathbb{R}$ defined by

$$\widehat{\zeta}(b) = \begin{cases} b^3 \ln(b^2) + b^5 - b^4, & \text{if} \quad b \neq 0 \\ 0, & \text{if} \quad b = 0 \end{cases},$$

we have $\widehat{u}_* = 1$ as a solution of $\widehat{\zeta}(b) = 0$. We also have $\widehat{\mathcal{P}}_0(\sigma) = \widehat{\mathcal{P}}(\sigma) = = 96.6629073\sigma$. For this problem, the parameters $\widehat{R}^*$ and $\kappa_m, m = 1, 4, 5$, are listed in Table 1.

Proposed Radius	Radius by Sharma and Parhi [23]
$\kappa_1 = 0.006896819941$	$R_1 = 0.006896$
$\kappa_4 = 0.006060095377$	$R_3 = 0.006060$
$\kappa_5 = 0.005948720195$	$R_5 = 0.004426$
$\widehat{R}^* = 0.005948720195$	$\widehat{R}^* = 0.004426$

Radius by Singh et al. [26]	Radius by Sharma and Parhi [24]
$r_1 = 0.006896$	$R_1 = 0.0045456$
$r_2 = 0.005172$	$R_3 = 0.003994$
$r_3 = 0.003317$	$R_5 = 0.002917$
$\widehat{R}^* = 0.003317$	$\widehat{R}^* = 002917$

Table 1. Radius of MWFM for Problem 1

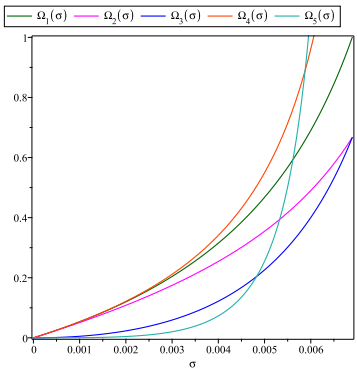

Figure 4. Ω_m, $m = 1, 2, \ldots, 5$, for Problem 1

Problem 2. [25, 7] By taking $\widetilde{\mathcal{D}}_1 = \widetilde{\mathcal{D}}_2 = C[0,1]$ and $\widetilde{\mathcal{D}} = P[\widehat{u}_*, 1]$, we define $\widehat{\zeta}$ for $b(\sigma) \in C[0,1]$ by

$$\widehat{\zeta}(b)(\sigma) = b(\sigma) - 5 \int_0^1 \sigma \ \upsilon \ b(\upsilon)^3 \ d\upsilon.$$

Nonlinear integral equations expressed in the form $\widehat{\zeta}(b)(\sigma) = 0$ fall under the category of Hammerstein-type equations. These Hammerstein equations frequently appear in a wide array of scientific applications, including the study of motion-related problems [14]. For the considered equation, we have $\widehat{u}_* = 0$. Also,

$$\widehat{\zeta}'(b(x))(\sigma) = x(\sigma) - 15 \int_0^1 \sigma \ \upsilon \ b(\upsilon)^2 \ x(\upsilon) \ d\upsilon, \ x \in \ \widetilde{\mathcal{D}},$$

and we have $\widehat{\zeta}'(\widehat{u}_*) = I$. Now, we obtain

$$\begin{aligned}
||\widehat{\zeta}'(\widehat{u}_*)^{-1}(\widehat{\zeta}'(b) - \widehat{\zeta}'(u))|| &\leq 15 \int_0^1 \upsilon ||b^2(\upsilon) - u^2(\upsilon)|| \ d\upsilon \leq \\
&\leq 15||b-u|| = \widehat{\mathcal{P}}(||b-u||), \ b, \ u \ \in \widetilde{\mathcal{D}}, \\
||\widehat{\zeta}'(\widehat{u}_*)^{-1}(\widehat{\zeta}'(b) - \widehat{\zeta}'(u_*))|| &\leq 15 \int_0^1 \upsilon ||b^2(\upsilon)|| \ d\upsilon \leq \\
&\leq 15 \int_0^1 \upsilon ||b|| \ ||b-u_*|| \ d\upsilon \leq \\
&\leq \frac{15}{2}||b-u_*|| = \widehat{\mathcal{P}}_0(||b-u_*||), \ b \ \in \widetilde{\mathcal{D}}.
\end{aligned}$$

Hence, $\widehat{\mathcal{P}}_0(\sigma) = 7.5\sigma$, and $\widehat{\mathcal{P}}(\sigma) = 15\sigma$. Table 2 contains the values of $\widehat{R}^*$ and $\kappa_m, m = 1, 4, 5$.

Proposed Radius	Radius by Sharma and Parhi [23]
$\kappa_1 = 0.06666666667$	$R_1 = 0.066667$
$\kappa_4 = 0.05333333333$	$R_3 = 0.053333$
$\kappa_5 = 0.05133383337$	$R_5 = 0.035647$
$\widehat{R}^* = 0.05133383337$	$\widehat{R}^* = 0.035647$

Radius by Singh et al. [26]	Radius by Sharma and Parhi [24]
$r_1 = 0.06667$	$R_1 = 0.066667$
$r_2 = 0.04185$	$R_3 = 0.053333$
$r_3 = 0.02481$	$R_5 = 0.035647$
$\widehat{R}^* = 0.02481$	$\widehat{R}^* = 0.035647$

Table 2. Radius of MWFM for Problem 2

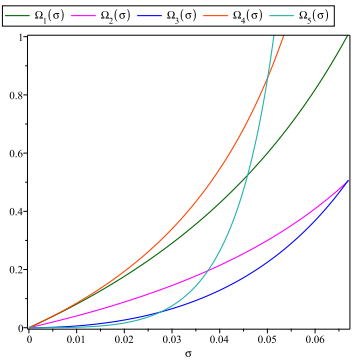

Figure 5. Ω_m, $m = 1, 2, \ldots, 5$, for Problem 2

Problem 3. [24] Let $\widetilde{\mathcal{D}}_1 = \widetilde{\mathcal{D}}_2 = \mathbb{R}^3$ and $\widetilde{\mathcal{D}} = P[\widehat{u}_*, 1]$. Define $\widehat{\zeta}$ for $b = (b_1, b_2, b_3)^t \in \widetilde{\mathcal{D}}$ by

$$\widehat{\zeta}(b) = (e^{b_1} - 1, \frac{e-1}{2} b_2^2 + b_2, b_3)^t.$$

For $\widehat{\zeta}(b) = 0$, the solution is $\widehat{u}_* = (0, 0, 0)^t$. We obtain $\widehat{\mathcal{P}}_0(\sigma) = 1.718281828\sigma$ and $\widehat{\mathcal{P}}(\sigma) = 1.789572397\sigma$. In Table 3, the parameters $\widehat{R}^*$ and $\kappa_m, m = 1, 4, 5$, are listed.

Proposed Radius	Radius by Sharma and Parhi [23]
$\kappa_1 = 0.3826919123$	$R_1 = 0.324947$
$\kappa_4 = 0.3345618308$	$R_3 = 0.268633$
$\kappa_5 = 0.3280809260$	$R_5 = 0.184350$
$\widehat{R}^* = 0.3280809260$	$\widehat{R}^* = 0.184350$

Radius by Singh et al. [26]	Radius by Sharma and Parhi [24]
$r_1 = 0.32495$	$R_1 = 0.324947$
$r_2 = 0.21657$	$R_3 = 0.268633$
$r_3 = 0.13125$	$R_5 = 0.184350$
$\widehat{R}^* = 0.13125$	$\widehat{R}^* = 0.184350$

Table 3. Radius of MWFM for Problem 3

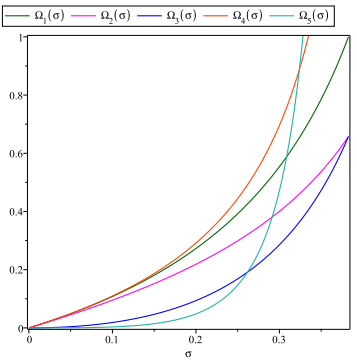

Figure 6. Ω_m, $m = 1, 2, \ldots, 5$, for Problem 3

Problem 4. [24] Suppose that $\widetilde{\mathcal{D}}_1 = \widetilde{\mathcal{D}}_2 = C[0,1]$ and $\widetilde{\mathcal{D}} = P[\widehat{u}_*, 1]$. We define $\widehat{\zeta}$ by

$$\widehat{\zeta}(b)(\sigma) = b(\sigma) - 3\int_0^1 \widetilde{A}(\sigma, \upsilon) b(\upsilon)^{\frac{5}{4}} d\upsilon,$$

where $b(\sigma) \in \widetilde{\mathcal{D}}$ and the Green's function $\widetilde{A}(\sigma, \upsilon)$ is defined on $[0,1] \times [0,1]$ by

$$\widetilde{A}(\sigma, \upsilon) = \begin{cases} (1-\sigma)\upsilon, & \text{if} \quad \upsilon \leq \sigma \\ \sigma(1-\upsilon), & \text{if} \quad \sigma \leq \upsilon. \end{cases}$$

The solution of $\widehat{\zeta}(b) = 0$ is $\widehat{u}_* = 0$, and we deduce that $\widehat{\mathcal{P}}_0(\sigma) = \widehat{\mathcal{P}}(\sigma) = \frac{15}{32}\sigma^{\frac{1}{4}}$. In Table 4, $\widehat{R}^*$ and $\kappa_m, m = 1, 4, 5$, are summarized.

Proposed Radius	Radius by Sharma and Parhi [23]
$\kappa_1 = 1.973080737$	$R_1 = **$
$\kappa_4 = 1.520540303$	$R_3 = **$
$\kappa_5 = 1.394150809$	$R_5 = **$
$\widehat{R}^* = 1.394150809$	$\widehat{R}^* = **$

Radius by Singh et al. [26]	Radius by Sharma and Parhi [24]
$r_1 = **$	$R_1 = 1.973080$
$r_2 = **$	$R_3 = 0.879329$
$r_3 = **$	$R_5 = 0.101198$
$\widehat{R}^* = **$	$\widehat{R}^* = 0.101198$

Table 4. Radius of MWFM for Problem 4

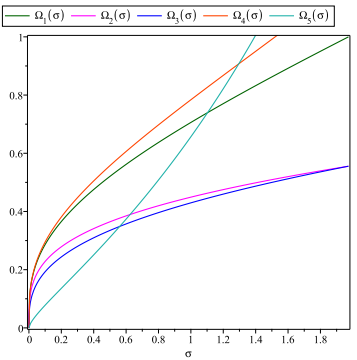

Figure 7. Ω_m, $m = 1, 2, \ldots, 5$, for Problem 4

Problem 5. [24] We take $\widetilde{\mathcal{D}}_1 = \widetilde{\mathcal{D}}_2 = C[0,1]$ and $\widetilde{\mathcal{D}} = P[\widehat{u}_*, 1]$, and the equation containing the integral operator as follows.

$$\widehat{\zeta}(b)(\sigma) = b(\sigma) - 5\int_0^1 \sigma\ \upsilon\ b(\upsilon)^{\frac{3}{2}} d\upsilon.$$

We obtain here $\widehat{u}_* = 0$, $\widehat{\mathcal{P}}_0(\sigma) = \widehat{\mathcal{P}}(\sigma) = \frac{15}{4}\sigma^{\frac{1}{2}}$. The radius $\widehat{R}^*$ and κ_m, $m = 1, 4, 5$, are placed in Table 5.

Proposed Radius	Radius by Sharma and Parhi [23]
$\kappa_1 = 0.02560$	$R_1 = **$
$\kappa_4 = 0.02094505672$	$R_3 = **$
$\kappa_5 = 0.01995840187$	$R_5 = **$
$\widehat{R}^* = 0.01995840187$	$\widehat{R}^* = **$

Radius by Singh et al. [26]	Radius by Sharma and Parhi [24]
$r_1 = **$	$R_1 = 0.025599$
$r_2 = **$	$R_3 = 0.017992$
$r_3 = **$	$R_5 = 0.007313$
$\widehat{R}^* = **$	$\widehat{R}^* = 0.007313$

Table 5. Radius of MWFM for Problem 5

In addition, we perform a comparative evaluation between MWFM and the classical Newton's method (NM) on Problems 1, 2, and 3 to thoroughly validate the convergence radii established for MWFM in this work. To solve the integral equation presented in Problem 2, we utilize the composite trapezoidal rule. The initial guesses are selected from within the convergence regions identified for MWFM, using the radii provided in Tables 1–3. All numerical tests are executed in MATLAB with variable precision arithmetic configured to 2000 digits. The termination condition is defined as $||\widehat{\zeta}(b_{s+1})|| + ||b_{s+1} - \widehat{u}_*|| < < 10^{-200}$. Results are listed in Tables 6–8, presenting the number of iterations (NI) needed to achieve the specified precision, the norm $||\widehat{\zeta}(b_{s+1})||$, and

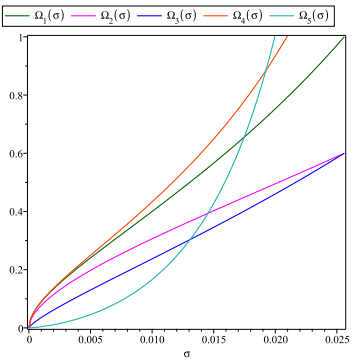

Figure 8. Ω_m, $m = 1, 2, \ldots, 5$, for Problem 5

the approximate computational order of convergence (ACOC), computed as $\left(ACOC = \frac{ln(||b_{s+1}-b_s||/||b_s-b_{s-1}||)}{ln(||b_s-b_{s-1}||/||b_{s-1}-b_{s-2}||)}\right)$ [25]. The findings indicate that MWFM consistently outperforms Newton's method in terms of iteration efficiency, accuracy, and ACOC. Consequently, the convergence of MWFM is confirmed through the strategic selection of initial points based on the radii analytically derived by our approach.

b_0	Methods	NI	$\|\|\widehat{\zeta}(b_{s+1})\|\|$	ACOC
0.995	NM	7	1.2×10^{-233}	2.0000
	MWFM	3	1.58×10^{-216}	4.9999
1.005	NM	7	1.01×10^{-234}	1.9999
	MWFM	3	8.37×10^{-218}	4.9999

Table 6. Comparison of MWFM with NM for Problem 1

b_0	Methods	NI
$[-0.0215,\ -0.0215,\ \ldots,\ -0.0215]^t$	NM	5
	MWFM	3
$[0.0225,\ 0.0225,\ 0.0225,\ 0.0225,\ 0.0225]^t$	NM	5
	MWFM	3

$\|\|\widehat{\zeta}(b_{s+1})\|\|$	ACOC
2.35×10^{-335}	3.0000
3.56×10^{-1044}	8.9999
1.50×10^{-330}	2.9999
9.23×10^{-1030}	9.0000

Table 7. Comparison of MWFM with NM for Problem 2

b_0	Methods	NI	$\|\|\widehat{\zeta}(b_{s+1})\|\|$	ACOC
$[-0.14,\ -0.14,\ -0.14]^t$	NM	8	6.96×10^{-222}	2.0000
	MWFM	4	2.04×10^{-491}	4.9999
$[0.18,\ 0.18,\ 0.18]^t$	NM	8	3.54×10^{-224}	2.0000
	MWFM	4	6.17×10^{-504}	4.9999

Table 8. Comparison of MWFM with NM for Problem 3

5. Conclusions

The proposed analysis significantly improves the convergence properties of the modified Weerakoon–Fernando iteration scheme (MWFM) by expanding its domain of convergence without imposing additional restrictive conditions. Through comprehensive theoretical analysis and supporting numerical experiments, the method has demonstrated greater reliability and effectiveness for solving nonlinear equations, particularly within Banach spaces. The investigation of attraction basins further confirms its robust performance and potential applicability to complex valued equations.

Availability of data and material. Data sharing is not applicable to this article as no datasets were generated or analyzed during the current study.

Conflict of interest. The authors declare that they have no competing interests.

References

[1] **Amat, S., I.K. Argyros, S. Busquier, M.A. Hernández-Verón and E. Martínez,** On the local convergence study for an efficient k-step iterative method, *J. Comput. Appl. Math.*, **343** (2018), 753–761. https://doi.org/10.1016/j.cam.2018.02.028

[2] **Argyros, I.K.,** *Convergence and Application of Newton-type Iterations*, Springer, 2008.

[3] **Argyros, I.K., R. Behl and S.S. Motsa,** Unifying semilocal and local convergence of Newton's method on Banach space with a convergence structure, *Appl. Numer. Math.*, **115** (2017), 225–234. https://doi.org/10.1016/j.apnum.2017.01.008

[4] **Argyros, I.K., Y.J. Cho and S. Hilout,** *Numerical Methods for Equations and its Applications*, Taylor & Francis, CRC Press, New York, 2012. https://doi.org/10.1201/b12297

[5] **Argyros, I.K., Y.J. Cho and S. George,** Local convergence for some third order iterative methods under weak conditions, *J. Korean Math. Soc.*, **53** (2016), 781–793.
https://doi.org/10.4134/JKMS.j150244

[6] **Argyros, I.K., S. George and Á.A. Magreñán,** Local convergence for multi-point-parametric Chebyshev–Halley–type methods of higher convergence order, *J. Comput. Appl. Math.*, **282** (2015), 215–224.
https://doi.org/10.1016/j.cam.2014.12.023

[7] **Argyros, I.K. and S. George,** Local convergence for an almost sixth order method for solving equations under weak conditions, *SeMA J.*, **75** (2017), 163–171.
https://doi.org/10.1007/s40324-017-0127-z

[8] **Argyros, I.K. and D. González,** Local convergence for an improved Jarratt-type method in Banach space, *Int. J. Interact. Multimed. Artif. Intell.*, **3** (2015), 20–25.
https://doi.org/10.9781/ijimai.2015.344

[9] **Argyros, I.K. and S. Hilout,** On the local convergence of fast two-step Newton-like methods for solving nonlinear equations, *J. Comput. Appl. Math.*, **245** (2013), 1–9.
https://doi.org/10.1016/j.cam.2012.12.002

[10] **Argyros, I.K. and Á.A. Magreñán,** A study on the local convergence and the dynamics of Chebyshev–Halley-type methods free from second derivative, *Numer. Algorithms*, **71** (2015), 1–23.
https://doi.org/10.1007/s11075-015-9981-x

[11] **Chang, C.W., S. Qureshi, I.K. Argyros, F.I. Chicharro and A. Soomro,** A modified two-step optimal iterative method for solving nonlinear models in one and higher dimensions, *Math. Comput. Simul.*, **229** (2025), 448–467.
https://doi.org/10.1016/j.matcom.2024.09.021

[12] **Cordero, A., J.A. Ezquerro, M.A. Hernández-Verón and J.R. Torregrosa,** On the local convergence of a fifth-order iterative method in Banach spaces, *Appl. Math. Comput.*, **251** (2015), 396–403.
https://doi.org/10.1016/j.amc.2014.11.084

[13] **Cordero, A., J.L. Hueso, E. Martínez and J.R. Torregrosa,** Increasing the convergence order of an iterative method for nonlinear systems, *Appl. Math. Lett.*, **25** (2012), 2369–2374.
https://doi.org/10.1016/j.aml.2012.07.005

[14] **Hernández-Verón, M.A., and E. Martínez,** On the semilocal convergence of a three steps Newton-type iterative process under mild convergence conditions, *Numer. Algorithms*, **70** (2015), 377–392.
https://doi.org/10.1007/s11075-014-9952-7

[15] **George, S., M. Muniyasamy, M. Gopal, G. Chandhini and I.K. Argyros,** A procedure for increasing the convergence order of iterative methods from p to $5p$ for solving nonlinear system, *J. Complexity*, **87** (2025), Article ID 101921.
https://doi.org/10.1016/j.jco.2024.101921

[16] **Kou, J., Y. Li and X. Wang,** A composite fourth-order iterative method for solving non-linear equations, *Appl. Math. Comput.*, **184** (2007), 471–475.
https://doi.org/10.1016/j.amc.2006.05.181

[17] **Martínez, E., S. Singh, J.L. Hueso and D.K. Gupta,** Enlarging the convergence domain in local convergence studies for iterative methods in Banach spaces, *Appl. Math. Comput.*, **281** (2016), 252–265.
https://doi.org/10.1016/j.amc.2016.01.036

[18] **Özban, A.Y.,** Some new variants of Newton's method, *Appl. Math. Lett.*, **17** (2004), 677–682.
https://doi.org/10.1016/S0893-9659(04)90104-8

[19] **Petković, M.S., B. Neta, L. Petković and D. Džunić,** *Multipoint methods for solving nonlinear equations*, Elsevier, Amsterdam, 2013.

[20] **Potra, F.A. and V. Pták,** Nondiscrete induction and iterative processes, *Pitman Publ., Boston, MA*, **103** (1984).

[21] **Regmi, S., I.K. Argyros, C.I. Argyros and D. Sharma,** Extended comparison between two derivative-free methods of order six for equations under the same conditions, *Fractal Fract.*, **6** (2022), Article No. 634.
https://doi.org/10.3390/fractalfract6110634

[22] **Scott, M., B. Neta and C. Chun,** Basin attractors for various methods, *Appl. Math. Comput.*, **218** (2011), 2584–2599.
https://doi.org/10.1016/j.amc.2011.07.076

[23] **Sharma, D. and S.K. Parhi,** On the local convergence of modified Weerakoon's method in Banach spaces, *J. Anal.*, **28** (2020), 867–877.
https://doi.org/10.1007/s41478-019-00216-x

[24] **Sharma, D. and S.K. Parhi,** On the local convergence of higher order methods in Banach spaces, *Fixed Point Theory*, **22** (2021), 855–870.
https://doi.org/10.24193/fpt-ro.2021.2.55

[25] **Sharma, J.R. and I.K. Argyros,** Local convergence of a Newton–Traub composition in Banach spaces, *SeMA J.*, **75** (2017), 57–68.
https://doi.org/10.1007/s40324-017-0113-5

[26] **Singh, S., E. Martínez, P. Maroju and R. Behl,** A study of the local convergence of a fifth order iterative method, *Indian J. Pure Appl. Math.*, **51** (2020), 439–455.
https://doi.org/10.1007/s13226-020-0409-5

[27] **Tassaddiq, A., S. Qureshi, I.K. Argyros, F.I. Chicharro, A. Soomro, P. Nizamani and E. Hincal,** A convergent and stable fourth-order iterative procedure based on Kung–Traub conjecture for nonlinear systems, *Appl. Numer. Math.*, **214** (2025), 54–79.
https://doi.org/10.1016/j.apnum.2025.03.003

[28] **Traub, J.F.,** *Iterative Methods for Solution of Equations*, Englewood Cliffs: Prentice-Hal, 1964.

[29] **Weerakoon S. and T.G.I. Fernando,** A variant of Newton's method with accelerated third-order convergence, *Appl. Math. Lett.*, **13** (2000), 87–93.
https://doi.org/10.1016/S0893-9659(00)00100-2

Ioannis K. Argyros
https://orcid.org/0000-0002-9189-9298
Department of Computing of Mathematical Sciences
Cameron University
Lawton, OK 73505
USA
iargyros@cameron.edu

Debasis Sharma
https://orcid.org/0000-0001-8456-6391
Department of Mathematics
Model Degree College
Rayagada
Odisha, 765017
India
iiit.debasis@gmail.com

Christopher Argyros
https://orcid.org/0000-0002-3758-9846
School of Computational Science and Engineering
Georgia Institute of Technology
225 North Avenue NW
Atlanta, GA 30313
USA
cargyros3@gatech.edu